3-17-2009

$La_{0.85}Sr_{0.15}MnO_{3-}$ Infiltrated $Y_{0.5}Bi_{1.5}O_3$ Cathodes for Intermediate-Temperature Solid Oxide Fuel Cells

Jiang Zhiyi
University of Science and Technology of China

Changrong Xia
University of Science and Technology of China

Fei Zhao
University of South Carolina - Columbia, zhaofei@cec.sc.edu

Fanglin Chen
University of South Carolina - Columbia, chenfa@cec.sc.edu

Publication Info

Electrochemical and Solid-State Letters, Volume 12, Issue 6, 2009, pages B91-B93.

Publisher's Version: http://dx.doi.org/10.1149/1.3099321
PACS: 82.47.Ed, 82.45.Fk, 82.45.Gj

Electrochemical and Solid-State Letters, **12** (6) B91-B93 (2009)
1099-0062/2009/12(6)/B91/3/$23.00 © The Electrochemical Society

$La_{0.85}Sr_{0.15}MnO_{3-\delta}$ Infiltrated $Y_{0.5}Bi_{1.5}O_3$ Cathodes for Intermediate-Temperature Solid Oxide Fuel Cells

Zhiyi Jiang,[a] Changrong Xia,[a,*,z] Fei Zhao,[a,b] and Fanglin Chen[b]

[a]*Laboratory for Renewable Clean Energy, Department of Materials Science and Engineering, University of Science and Technology of China, Hefei, 230026 Anhui, China*
[b]*Department of Mechanical Engineering, University of South Carolina, Columbia, South Carolina 29208, USA*

Porous yttria-stabilized bismuth oxides (YSB) were investigated as the backbones for $La_{0.85}Sr_{0.15}MnO_{3-\delta}$ (LSM) infiltrated cathodes in intermediate-temperature solid oxide fuel cells. The cathodes were evaluated using anode-supported single cells with scandia-stabilized zirconia as the electrolytes. With humidified H_2 as the fuel, the cell showed peak power density of 0.33, 0.52, and 0.74 W cm^{-2} at 650, 700, and 750°C, respectively. At 650°C, the cell polarization resistance was only 1.38 Ω cm^2, <50% of the lowest value previously reported, indicating that YSB is a promising backbone for the LSM infiltrated cathode.
 [DOI: 10.1149/1.3099321]

Manuscript submitted December 18, 2008; revised manuscript received February 23, 2009. Published March 17, 2009.

Electrode polarization loss of the $(La,Sr)MnO_3$ (LSM) cathode dominates the total cell polarization loss of solid oxide fuel cells (SOFCs) operating at intermediate temperatures (600–800°C).[1,2] To reduce the cell polarization loss and thus improve the cell performance, LSM is usually cooperated with oxygen-ion conductors, such as stabilized zirconia and doped ceria, to form a composite cathode, which is believed to have prolonged three-phase boundaries (TPBs) for the electrochemical reduction of oxygen.[2-5]

Cathode constructed by infiltrating LSM nanoparticles into a preformed porous yttria-stabilized zirconia (YSZ) backbone has demonstrated lower polarization loss than composite cathode formed by randomly distributed YSZ and LSM particles.[6,7] Because of its unique microstructure, the cathode prepared by the infiltration approach has at least three advantages compared to the composite cathode. First, the LSM electrocatalyst is of nanoscale, which is favorable to the catalytic activity. Second, good electronic conductivity is easy to achieve in the infiltrated cathode even when the LSM loading is well below the percolation threshold needed in a randomly packed composite cathode structure. A single LSM infiltration step has been shown enough to assure good electronic conductivity.[7] Finally, the well-sintered ionic-conducting backbone assures a consecutive ionic-conduction pathway, which increases the TPB sites, where oxygen ions, electrons, and gas (oxygen) meet. Consequently, high electrode performance is expected for a backbone with high oxygen-ion conductivity.

Stabilized bismuth oxide is expected to be a superior material for the cathode backbone due to its much higher oxide ionic conductivity than that of YSZ.[8] The oxides have been used as electrolyte components in combination with Ag to form composite cathodes in which the oxides and Ag are randomly distributed.[9,10] In addition, cathodes consisting of nanosized yttria-stabilized bismuth oxide (YSB) and porous LSM backbones have been previously prepared by infiltrating YSB solutions into LSM backbones and have exhibited very high performances as the cathodes for intermediate-temperature SOFCs with doped ceria and YSZ as the electrolytes.[11,12] In this work, bismuth oxide is evaluated as the porous backbone to cooperate with LSM nanoelectrocatalyst as the cathodes for intermediate-temperature SOFCs.

Experimental

Anode and electrolyte were donated by Shanghai Institute of Ceramics, Chinese Academy of Science. The anode and electrolyte were prepared by multilayer tape casting and cosintering at 1400°C for 4 h.[13] The resulting multilayer structure consisted of a 600 μm thick anode substrate (NiO and 50 wt % $Zr_{0.92}Y_{0.08}O_{2-\delta}$), a 15 μm thick anode functional layer (NiO and 50 wt % $Zr_{0.89}Sc_{0.1}Ce_{0.01}O_{2-\delta}$), a 15 μm thick $Zr_{0.89}Sc_{0.1}Ce_{0.01}O_{2-x}$ electrolyte, and a 10 μm thick $Ce_{0.8}Gd_{0.2}O_{1.9}$ (GDC) interlayer. To fabricate the porous backbone, YSB powder was synthesized using a glycine-nitrate process with $Bi(NO_3)_3$, $Y(NO_3)_3$, and glycine as starting materials. The YSB backbone was fabricated by brush printing YSB slurry (composed of YSB, starch, and terpineol at 70:30:150 weight ratio) on the top of the GDC interlayer. It was then dried and fired at 850°C for 2 h. The thickness of the YSB backbone was ~50 μm. Coating of the LSM nanoparticles in the YSB backbone was conducted by an impregnation process. A solution containing $La(NO_3)_3$, $Sr(NO_3)_2$, and $Mn(NO_3)_2$ (La^{3+}:Sr^{2+}:Mn^{2+} = 85:15:100) and glycine (added as a complexing agent and with a concentration half of that of the nitrate ions) was dropped onto the top of YSB layer. The sample was dried at room temperature and then heated at 800°C for 2 h to form LSM nanoparticles. After one impregnation-heating step, the weight ratio of LSM to YSB was 16:84. LSM powder was also prepared from the above solution through the glycine nitrate process for X-ray diffraction (XRD) characterization.

Electrochemical performance of the fuel cell was tested at 650, 700, and 750°C using a Zahner Im6e electrochemical workstation. Ag paste was printed on the cathode surface to assure good electronic contact. The anode was fueled with humidified H_2 (3% H_2O) at a flow rate of 100 mL min^{-1}, and the cathode was exposed to ambient air. Impedance spectra were recorded in a frequency range of 1 MHz to 100 mHz with an ac perturbation signal of 10 mV. Crystalline structures and phases of the samples were characterized by XRD, MXPAHF with Cu Kα radiation in the 2θ range of 20–80°. Microstructure analysis was performed using a scanning electron microscope [(SEM), JEOL JSM-6700F and FEI Sirion200].

Results and Discussion

XRD pattern of a free standing YSB backbone infiltrated with LSM particles as well as those of the YSB and LSM powders are shown in Fig. 1. Perovskite LSM was formed when the impregnated nitrates were heated at 800°C for 2 h. No obvious reaction between LSM and YSB was observed, and the impregnation process did not introduce any other unexpected phases.

Shown in Fig. 2 are the SEM images of the YSB backbone and the LSM infiltrated YSB cathode before and after electrochemical testing. Figure 2a shows that almost no particle boundary is observed on the sintered YSB backbone, a characteristic favorable to the oxygen-ion transport. After impregnation and heating, LSM particles with ~100 nm diam have formed a porous coating layer on the surface of the YSB backbone, as shown in Fig. 2b. This microstructure is very similar to those of infiltrated cathodes previously reported.[7,14] The porosity of the YSB backbone is estimated to be ~49% from the analysis of the SEM images. The porosity drops to

* Electrochemical Society Active Member.
z E-mail: xiacr@ustc.edu.cn

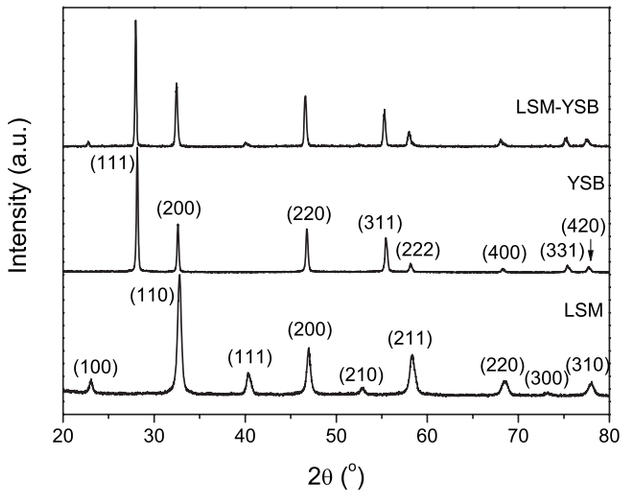

Figure 1. XRD patterns of the LSM infiltrated YSB backbone and YSB and LSM powders.

~36% when the LSM is infiltrated in the YSB backbone. After testing over 300 h, a slight increase in the LSM particle size is observed while the LSM layer remains porous, as shown in Fig. 2c.

Shown in Fig. 3a are the cell power output performances using humidified hydrogen as the fuel. The power density increases with the increase in the cell operating temperature. The peak power densities are 0.33, 0.52, and 0.74 W cm^{-2} at 650, 700, and 750°C, respectively. The power density at 650°C in this work is >20% higher than the value previously reported (0.27 W cm^{-2}) for a cell with LSM infiltrated YSZ backbone as cathode.[7] Figure 3b shows the cell durability performance with the power density as a function of the operating time when the cell was operated at 0.7 V and 700°C. The power density declined fairly fast, from 0.39 to 0.33 W cm^{-2} during the initial 50 h, but was then gradually stabilized in the subsequent 100 h. A 700°C-to-room-temperature thermal cycle was conducted after the cell was operated at 0.7 V for 143 h. Following the thermal cycle, the power density increased to 0.36 W cm^{-2} and was relatively stable, subsequently, for over 150 h. The initial power decline might be attributed to the coarsening of the LSM particles as revealed by the SEM observations (Fig. 2c). Similar behavior was previously reported for $La_{0.8}Sr_{0.2}FeO_3$-infiltrated YSZ cathode.[14] The coarsening of the infiltrated particles is very likely to be inevitable because small particle size usually results in high sinterability. However, the particle growth seems to be self-limited, and the coarsening would be gradually suppressed. Because the LSM particles formed a thin and porous layer on the surface of the YSB backbone, the packing of LSM particles is quasi-two-dimensional. Thus, the growth of LSM particles is consequently limited by the supply of LSM substance. A similar phenomenon is previously observed on $Sm_{0.5}Sr_{0.5}CoO_3$ electrodes infiltrated onto ceria backbones.[15] In addition, during the long-term operation, the cathode was under cathodic polarization, which would lead to the elimination of the cation vacancies at the A sites of the LSM crystalline lattice.[16] The elimination of the cation vacancies hinders the diffusion of the cation ions. Consequently, the sintering of particles was suppressed, and the power output of the cell became stable over time.

Shown in Fig. 4a are the impedance spectra of the cell recorded at various operating temperatures. The total cell polarization resistances were 1.38, 0.94, and 0.68 Ω cm^2 at 650, 700, 750°C, respectively. As shown in Fig. 4b, the total cell polarization resistances in this work are among the lowest values for SOFCs with the LSM-based cathodes.[7,17-21] Specifically, at 650°C, the cell polarization resistance is <50% of the previously reported value obtained in an SOFC with the LSM-infiltrated YSZ backbone as a cathode.[7] Because the cathode polarization dominates the total cell polarization resistance at temperature of <750°C,[22-24] the result indicates that LSM-infiltrated cathode with the YSB backbone shows better performance than that with YSZ backbone. The performance improvement is probably related to the much higher ionic conductivity of YSB.

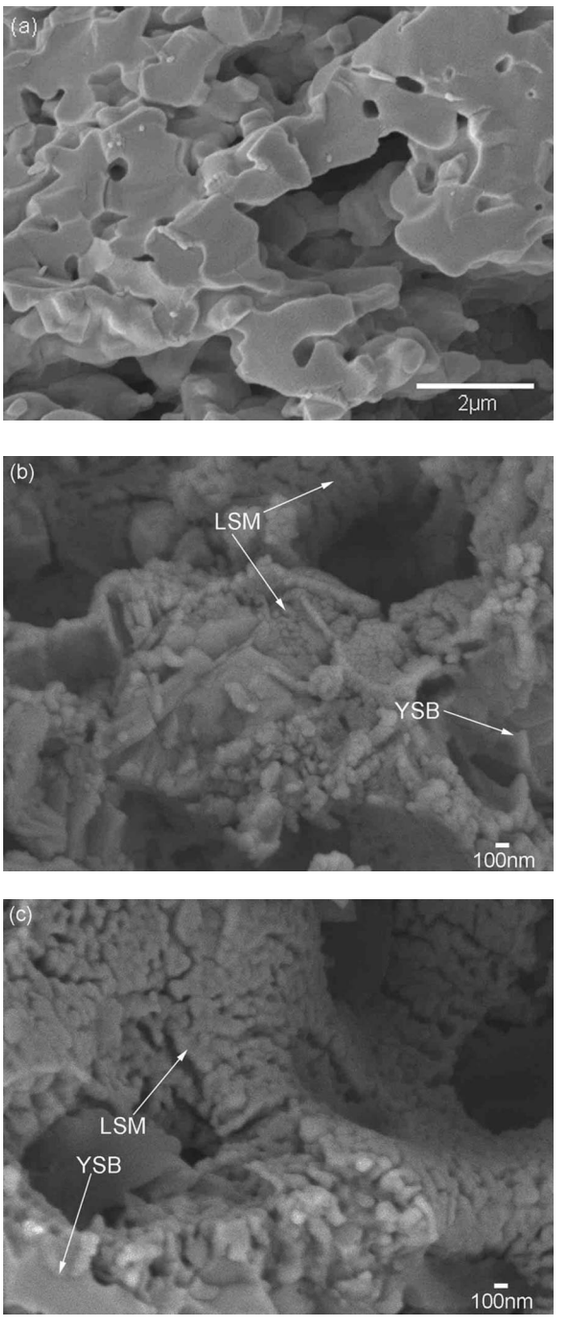

Figure 2. Cross-sectional images of (a) YSB backbone, (b) as-prepared LSM-infiltrated YSB backbone, and (c) LSM-infiltrated YSB backbone cathode after 300 h testing.

Conclusion

YSB was evaluated as the backbone for the LSM-infiltrated cathodes for SOFCs. The power output of the anode-supported single cell with the LSM-infiltrated YSB backbone as the cathode is higher than that of a single cell with the LSM-infiltrated YSZ backbone as

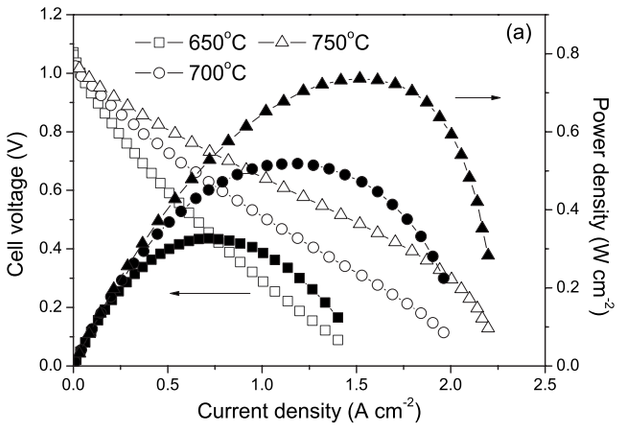

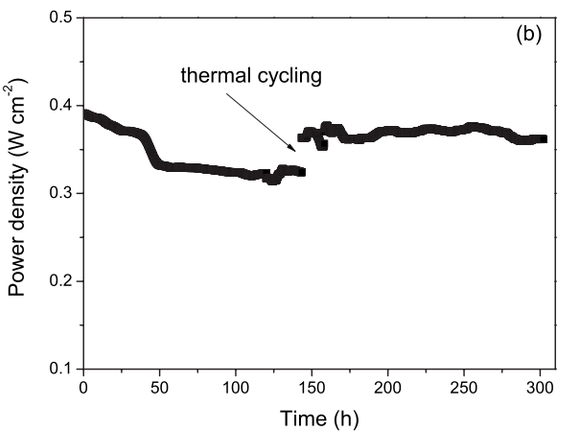

Figure 3. (a) Power density and voltage as a function of current density at 650, 700, and 750°C and (b) power output at 0.7 V and 700°C as a function of time for the cell with LSM-infiltrated YSB backbone as the cathode.

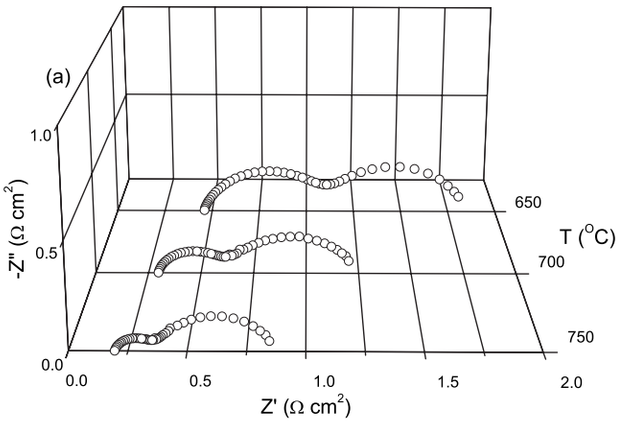

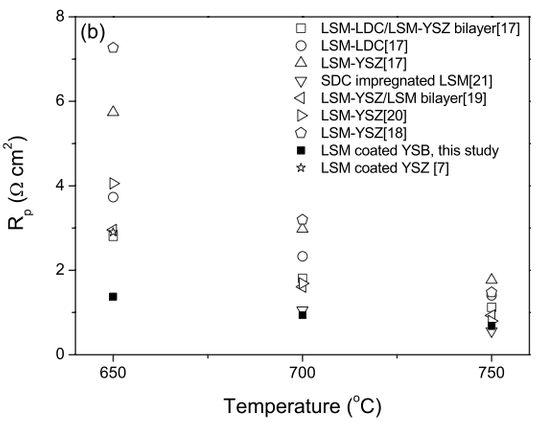

Figure 4. (a) Impedance spectra recorded under open circuit at 650–750°C for the cell with LSM-infiltrated YSB backbone cathode and (b) comparison of the total cell resistances for the cells with LSM-based cathodes.

the cathode previously reported. The cell polarization resistance for an SOFC with the LSM-infiltrated YSZ backbone as the cathode is the lowest among all the reported SOFCs with the LSM-based cathodes at operating temperatures of 700°C and below.

Acknowledgments

We thank Shanghai Institute of Ceramics for providing the multilayer anode-supported electrolyte samples. Financial support by the Natural Science Foundation of China (grant no. 50672096 and no. 50730002), the Ministry of Science and Technology of China (grant no. 2007AA05Z151), and the U.S. Department of Energy (DE-FG36-08GO88116) are greatly appreciated.

University of Science and Technology of China assisted in meeting the publication costs of this article.

References

1. S. B. Adler, *Chem. Rev. (Washington, D.C.)*, **104**, 4791 (2004).
2. T. J. Armstrong and A. V. Virkar, *J. Electrochem. Soc.*, **149**, A1565 (2002).
3. T. Kenjo, S. Osawa, and K. Fujikawa, *J. Electrochem. Soc.*, **138**, 349 (1991).
4. E. P. Murray and S. A. Barnett, *Solid State Ionics*, **143**, 265 (2001).
5. S. P. Jiang and W. Wang, *J. Electrochem. Soc.*, **152**, A1398 (2005).
6. Y. Y. Huang, J. M. Vohs, and R. J. Gorte, *J. Electrochem. Soc.*, **152**, A1347 (2005).
7. T. Z. Sholklapper, C. Lu, C. P. Jacobson, S. J. Visco, and L. C. De Jonghe, *Electrochem. Solid-State Lett.*, **9**, A376 (2006).
8. N. M. Sammes, G. A. Tompsett, H. Nafe, and F. Aldinger, *J. Eur. Ceram. Soc.*, **19**, 1801 (1999).
9. C. R. Xia, Y. Zhang, and M. L. Liu, *Appl. Phys. Lett.*, **82**, 901 (2003).
10. A. Jaiswal and E. D. Wachsman, *Solid State Ionics*, **177**, 677 (2006).
11. Z. Y. Jiang, L. Zhang, K. Feng, and C. R. Xia, *J. Power Sources*, **185**, 40 (2008).
12. Z. Y. Jiang, L. Zhang, L. L. Cai, and C. R. Xia, *Electrochim. Acta*, **54**, 3059 (2009).
13. Z. R. Wang, J. Q. Qian, H. D. Cao, S. R. Wang, and T. L. Wen, *J. Alloys Compd.*, **437**, 264 (2007).
14. W. S. Wang, M. D. Gross, J. M. Vohs, and R. J. Gorte, *J. Electrochem. Soc.*, **154**, B439 (2007).
15. F. Zhao, Z. Y. Wang, M. F. Liu, L. Zhang, C. R. Xia, and F. L. Chen, *J. Power Sources*, **185**, 13 (2008).
16. S. P. Jiang and W. Wang, *Solid State Ionics*, **176**, 1185 (2005).
17. M. Zhang, M. Yang, Z. F. Hou, Y. L. Dong, and M. J. Cheng, *Electrochim. Acta*, **53**, 4998 (2008).
18. Y. J. Leng, S. H. Chan, K. A. Khor, and S. P. Jiang, *Int. J. Hydrogen Energy*, **29**, 1025 (2004).
19. T. L. Reitz and H. M. Xiao, *J. Power Sources*, **161**, 437 (2006).
20. L. Zhang, S. P. Jiang, W. Wang, and Y. J. Zhang, *J. Power Sources*, **170**, 55 (2007).
21. J. M. Wang, Z. Lu, X. Q. Huang, K. F. Chen, N. Ai, J. Y. Hu, and W. H. Su, *J. Power Sources*, **163**, 957 (2007).
22. T. Tsai and S. A. Barnett, *Solid State Ionics*, **93**, 207 (1997).
23. C. R. Xia and M. L. Liu, *Solid State Ionics*, **144**, 249 (2001).
24. S. deSouza, S. J. Visco, and L. C. DeJonghe, *Solid State Ionics*, **98**, 57 (1997).